Laser and Particle Beams (2012), *30*, 281–289.

doi:10.1017/S0263034612000079

Betatron radiation damping in laser plasma acceleration

AIHUA DENG,[1] KAZUHISA NAKAJIMA,[1,2,3] XIAOMEI ZHANG,[1] HAIYANG LU,[1] BAIFEI SHEN,[1] JIANSHENG LIU,[1] RUXIN LI,[1] AND ZHIZHAN XU[1]

[1]Shanghai Institute of Optics and Fine Mechanics, CAS, Shanghai, China
[2]High Energy Accelerator Research Organization, Tsukuba, Ibaraki, Japan
[3]Shanghai Jiao Tong University, Shanghai, China

(RECEIVED 12 October 2011; ACCEPTED 13 February 2012)

Abstract

We explore the feasibility of accelerating electron beams up to energies much beyond 1 TeV in a realistic scale and evolution of the beam qualities such as emittance and energy spread at the final beam energy on the order of 100 TeV, using the newly formulated coupled equations describing the beam dynamics and radiative damping of electrons. As an example, we present a design for a 100 TeV laser-plasma accelerator in the operating plasma density $n_p = 10^{15}$ cm^{-3} and numerical solutions for evolution of the normalized emittance as well as their analytical solutions. We show that the betatron radiative damping causes very small normalized emittance that promises future applications for the high-energy frontier physics.

Keywords: Betatron oscillation; Laser wakefields; Laser-plasma accelerators; Radiative damping; TeV linear collider

1. INTRODUCTION

In this decade, vital researches on laser-driven plasma-based acceleration of charged particles have achieved great progress in high-energy, high-quality electron beams with energies of GeV-level (Leemans *et al.*, 2006; Clayton *et al.*, 2010; Lu *et al.*, 2011), qualities of 1%-level energy spread (Kameshima *et al.*, 2008), 1-mm-mrad-level transverse emittance (Karsch *et al.*, 2007), and 1-fs-level bunch duration (Lundh *et al.*, 2011), ensuring that the stability of reproduction is as high as that of present high-power ultra-short-pulse lasers (Osterhoff *et al.*, 2008; Hafz *et al.*, 2008). These high-energy high-quality particle beams make it possible to open the door for a wide range of applications in fundamental researches, medical, and industrial uses. For many applications of laser wakefields accelerators, stability and controllability of the beam performance such as beam energy, energy spread, emittance, and charge are indispensable as well as compact and robust features of the system. In particular, there are great interests in applications for high energy physics and astrophysics that explore unprecedented high-energy frontier phenomena much beyond 1 TeV, for which laser-plasma accelerator concepts provide us with promising tools if beam-quality issues are figured out as well as an achievable highest energy.

Address correspondence and reprint request to: Aihua Deng, Shanghai Institute of Optics and Fine Mechanics, CAS, Shanghai 201800, China. E-mail: aihuadeng@siom.ac.cn and nakajima@post.kek.jp

To date, most of experimental results have been obtained from interaction of ultra-short laser pulses, $\tau_L = 30 - 80$ fs with a short-scale plasma such as a few mm long gas jet and a few centimeter long plasma channel at the plasma density in the range of $n_p = 10^{18} - 10^{19}$ cm^{-3}, where a large amplitude plasma wave on the order of 100 GV/m is excited and likely candidates for the next generation of compact accelerators (Nakajima, 2000; Malka, 2002; Weber *et al.*, 2004). The leading experiments that demonstrated the production of quasi-monoenergetic electron beams (Mangles *et al.*, 2004; Geddes *et al.*, 2004; Faure *et al.*, 2004; Glinec *et al.*, 2005), have been elucidated in terms of self-injection and successive acceleration of electrons in the nonlinear wakefield, referred to as a "bubble" that is a region where plasma electrons are blown out by radiation pressure of a laser pulse with the relativistic intensity given by its normalized vector potential $a_L = eA_L/mc^2 \gg 1$, where A_L is the peak amplitude of the vector potential and mc^2 is the rest energy of electron (Kostyukov *et al.*, 2004; Lu *et al.*, 2006). The self-injection is a robust method relying on self-focusing and self-compression that occur during the propagation of relativistic laser pulses. In this mechanism, initially heated electrons with large transverse momentum are injected into nonlinear wakefields that excite betatron oscillation of accelerated electrons due to strong focusing field. Hence, suppressing the self-injection and the deterioration of beam qualities, high-quality electron beams required for most of applications have been produced with controlled injection schemes,

such as colliding optical injection (Faure *et al.*, 2006; Kotaki *et al.*, 2009; Wang *et al.*, 2009), density-transition injection (Schmid *et al.*, 2010), and ionization-induced injection (Pak *et al.*, 2010; McGuffey *et al.*, 2010), in the quasi-linear regime of wakefields driven by a laser pulse with a moderate intensity $a_L \sim 1$. These injection schemes provide us with high-quality electron beam injectors for a front end of the multi-stage laser-plasma accelerators, aiming at the high-energy frontier. Recently, two-stage laser-plasma acceleration has been successfully demonstrated in combination with ionization-induced injection (Liu *et al.*, 2011; Pollock *et al.*, 2011). Based on recent results of vital experiments and large-scale particle-in-cell simulations (Martins *et al.*, 2010), the design considerations and the feasibility studies on applications for high-energy frontier collider with the TeV-class center-of-mass energy have been carried out (Schroeder *et al.*, 2010; Nakajima *et al.*, 2011). In these considerations, the most critical issue is a choice of the operating plasma density that is an underlying parameter controlling the size, the performance, and the beam dynamics. Generally speaking, from the viewpoint of the beam qualities, the higher energy regime is in favor of the lower operating density, although such option leads to a larger size and a higher laser peak power. In laser plasma acceleration, electrons are accelerated by the ultra-high gradients on the order of 10–100 GV/m and undergo the strong transverse focusing force with the same order of the accelerating force. Initially heated electrons with large transverse momentum are injected and accelerated in plasma waves, and exhibit the betatron oscillation that generates the emission of intense synchrotron radiation. On one hand, the intense betatron radiation from laser-plasma accelerated electrons is an attractive X-ray/gamma-ray radiation source and on the other hand, it produces a radiation loss of the beam energy and a significant effect on the beam qualities such as the energy spread and the transverse emittance via the radiation reaction force (Michel *et al.*, 2006).

Here we consider the feasibility of accelerating electron beams up to energies much beyond 1 TeV and evolution of the beam qualities such as emittance and energy spread at the final beam energy. First we review the scaling formulas for designing laser-plasma accelerators in the quasi-linear laser wakefield regime, and work out the basic equations describing evolution of the normalized transverse emittance and the energy spread, taking into account radiative damping due to the betatron oscillation of electrons that undergo strong acceleration and focusing forces simultaneously. As an example, we present the parameters for 100 TeV laser-plasma linac in the operating plasma density $n_p = 10^{15}\ \mathrm{cm}^{-3}$ and numerical solutions for evolution of the normalized emittance and the energy spread as well as their analytical solutions. We show that the betatron radiative damping causes a very small normalized emittance that promises future applications for the high-energy frontier physics.

2. LASER-PLASMA ACCELERATORS

In underdense plasma, an ultra-intense laser pulse excites a large-amplitude plasma wave with frequency $\omega_p = \sqrt{4\pi e^2 n_p/m}$ and electric field of the order of

$$E_0 = \frac{mc\omega_p}{e} \simeq 96[\mathrm{GV/m}]\left(\frac{n_p}{10^{18}[\mathrm{cm}^{-3}]}\right)^{1/2}, \quad (1)$$

for the plasma density n_p due to the ponderomotive force expelling plasma electrons out of the laser pulse, and the space charge force of immovable plasma ions restoring expelled electrons on the back of the ion column remaining behind the laser pulse. Since the phase velocity of the plasma wave is approximately equal to the group velocity of the laser pulse $v_p/c \simeq \sqrt{1-\omega_p^2/\omega_L^2} \approx 1$ for the laser frequency ω_L and the accelerating field of about 100 GV/m for the plasma density $n_p \sim 10^{18}\ \mathrm{cm}^{-3}$, electrons trapped into the plasma wave are likely to be accelerated up to about 1 GeV energy in a 1-cm plasma.

In the quasi-linear laser wakefield regime, the normalized laser intensity,

$$a_L = \left(\frac{2e^2\lambda_L^2 I_L}{\pi m^2 c^5}\right)^{1/2} \simeq 0.855\times 10^{-9} I_L^{1/2}[\mathrm{W/cm}^2]\lambda_L[\mu\mathrm{m}], \quad (2)$$

is set to be $a_L \approx 1$, where I_L is the laser intensity and $\lambda_L = 2\pi c/\omega_L$ is the laser wavelength. In this regime, the wake potential Φ is obtained by

$$\frac{\partial^2\Phi}{\partial\zeta^2} + k_p^2\Phi = \frac{1}{2}k_p^2 mc^2 a^2(r,\zeta), \quad (3)$$

where $\zeta = z - v_p t$, $k_p = \omega_p/c$ and $a(r,\zeta) \equiv eA(r,\zeta)/mc^2$ is the normalized vector potential of the laser pulse. The wake potential is calculated by

$$\Phi(r,\zeta) = -\frac{m_e c^2 k_p}{2}\int_\zeta^\infty d\zeta' \sin k_p(\zeta-\zeta')a^2(r,\zeta'), \quad (4)$$

and the axial and radial electric fields are obtained by

$$eE_z = -\frac{\partial\Phi}{\partial z}, \quad \text{and} \quad eE_r = -\frac{\partial\Phi}{\partial r}, \quad (5)$$

respectively. Considering a bi-Gaussian laser pulse with $1/e$ half-width σ_L and $1/e^2$ spot radius r_L, of which the ponderomotive potential is given by

$$a^2(r,\zeta) = \frac{a_L^2}{2}\exp\left(-\frac{2r^2}{r_L^2} - \frac{\zeta^2}{\sigma_L^2}\right), \quad (6)$$

Behind the laser pulse at $\zeta \ll -\sigma_L$, the axial and radial

https://doi.org/10.1017/S0263034612000079 Published online by Cambridge University Press

wakefields are

$$E_z(r,\zeta) = \frac{\sqrt{\pi}}{4} a_L^2 k_p \sigma_L E_0 \exp\left(-\frac{2r^2}{r_L^2} - \frac{k_p^2\sigma_L^2}{4}\right)\cos k_p\zeta, \quad (7)$$

and

$$E_r(r,\zeta) = -\sqrt{\pi} a_L^2 \frac{\sigma_L r}{r_L^2} E_0 \exp\left(-\frac{2r^2}{r_L^2} - \frac{k_p^2\sigma_L^2}{4}\right)\sin k_p\zeta, \quad (8)$$

respectively. Setting $k_p\sigma_L = 1$, i.e., the full width at half maximum (FWHM) pulse length, $c\tau_L = 2\sqrt{\ln 2}\sigma_L \approx 0.265\lambda_p$, the maximum accelerating field is

$$E_{z\max} \approx 0.35 a_L^2 E_0 \simeq 1.06[\mathrm{GV/m}] a_L^2 \left(\frac{n_p}{10^{15}[\mathrm{cm}^{-3}]}\right)^{1/2}. \quad (9)$$

In this condition, the laser pulse length is shorter enough than a half plasma wavelength so that a transverse field at the tail of the laser pulse is negligible in the accelerating phase of the first wakefield. The net accelerating field E_z that accelerates the bunch containing the charge $Q_b = eN_b$, where N_b is the number of electrons in the bunch, is determined by the beam loading that means the energy absorbed per unit length,

$$Q_b E_z = \frac{mc^2}{4r_e} k_p^2 \sigma_r^2 \frac{E_{z\max}^2}{E_0^2}\left(1 - \frac{E_z^2}{E_{z\max}^2}\right), \quad (10)$$

where $r_e = e^2/mc^2$ is the classical electron radius and $1 - E_z^2/E_{z\max}^2 \equiv \eta_b$ is the beam loading efficiency that is the fraction of the plasma wave energy absorbed by particles of the bunch with the rms radius σ_r. In the beam-loaded field $E_z = \sqrt{1-\eta_b}E_{z\max}$, the charge is obtained as

$$\begin{aligned} Q_b &\simeq \frac{e}{4k_L r_e}\frac{\eta_b k_p^2\sigma_r^2}{(1-\eta_b)}\frac{E_z}{E_0}\left(\frac{n_c}{n_p}\right)^{1/2} \\ &\approx 2.4[\mathrm{nC}]\frac{\eta_b k_p^2\sigma_r^2}{(1-\eta_b)}\frac{E_z}{E_0}\left(\frac{n_p}{10^{15}[\mathrm{cm}^{-3}]}\right)^{-1/2}, \end{aligned} \quad (11)$$

where $n_c = m\omega_L^2/4\pi e^2 = \pi/(r_e\lambda_L^2) \approx 1.115\times 10^{21}$ $[\mathrm{cm}^{-3}]$ $(\lambda_L[\mu\mathrm{m}])^{-2}$ is the critical plasma density and for $k_p\sigma_L = 1$, $E_z/E_0 \simeq 0.35 a_0^2\sqrt{1-\eta_b}$. Since the loaded charge depends on the accelerating field and the bunch radius, it will be determined by considering the required accelerating gradient and the transverse beam dynamics.

First we consider a design of multi-TeV linear accelerators composed of multi-staging TeV laser-plasma accelerators, each of which can provide a single-stage energy gain of 1 TeV in a relatively compact scale. Ideally, the stage length L_{stage} is limited by the pump depletion length L_{pd} for which the total field energy is equal to half the initial laser energy. For a Gaussian laser pulse with pulse length $k_p\,\sigma_L = 1$, the pump depletion length is given by

$$k_p L_{\mathrm{pd}} \simeq \frac{8}{\sqrt{\pi}a_L^2 k_p\sigma_L}\frac{\omega_L^2}{\omega_p^2}\exp\left(\frac{k_p^2\sigma_L^2}{2}\right) \approx \frac{7.4}{a_L^2}\frac{n_c}{n_p}. \quad (12)$$

In laser wakefield accelerators, accelerated electrons eventually overrun the acceleration phase to the deceleration phase, of which the velocity is approximately equal to the group velocity of the laser pulse. In the linear wakefield regime, the dephasing length L_{dp} where the electrons undergo both focusing and acceleration is approximately given by

$$k_p L_{\mathrm{dp}} \simeq \pi\frac{\omega_L^2}{\omega_p^2} = \pi\frac{n_c}{n_p}. \quad (13)$$

In the condition for the dephasing length less than the pump depletion length, $L_{\mathrm{dp}} \le L_{\mathrm{pd}}$, the normalized vector potential should be $a_L \le 1.5$. Setting $a_L = 1.5$, the maximum accelerating field is $E_{z\max} \approx 0.79E_0$ for $k_p\sigma_L = 1$. Assuming the beam-loaded efficiency $\eta_b = 0.5$, the net accelerating field becomes

$$E_z \approx \frac{E_{z\max}}{\sqrt{2}} \simeq 0.56E_0 \approx 1.69[\mathrm{GV/m}]\left(\frac{n_p}{10^{15}[\mathrm{cm}^{-3}]}\right)^{1/2}. \quad (14)$$

For the stage length approximately equal to the dephasing length,

$$\begin{aligned} L_{\mathrm{stage}} \approx L_{\mathrm{dp}} &= \frac{\lambda_p}{2}\frac{n_c}{n_p} = \frac{\lambda_L}{2}\left(\frac{n_c}{n_p}\right)^{3/2} \\ &\approx 589[\mathrm{m}]\left(\frac{1[\mu\mathrm{m}]}{\lambda_L}\right)^2\left(\frac{10^{15}[\mathrm{cm}^{-3}]}{n_p}\right)^{3/2}, \end{aligned} \quad (15)$$

and the accelerating field Eq. (14), the energy gain per stage is given by

$$\begin{aligned} W_{\mathrm{stage}} = E_z L_{\mathrm{stage}} &= \pi mc^2\frac{E_z}{E_0}\frac{n_c}{n_p} \\ &\approx 1[\mathrm{TeV}]\frac{10^{15}[\mathrm{cm}^{-3}]}{n_p}\left(\frac{1[\mu\mathrm{m}]}{\lambda_L}\right)^2. \end{aligned} \quad (16)$$

The total number of stages becomes

$$\begin{aligned} N_{\mathrm{stage}} \simeq \frac{E_b}{W_{\mathrm{stage}}} &= \frac{\gamma_f}{\pi}\left(\frac{E_z}{E_0}\right)^{-1}\left(\frac{n_c}{n_p}\right)^{-1} \\ &\approx \frac{E_b}{1[\mathrm{TeV}]}\frac{n_p}{10^{15}[\mathrm{cm}^{-3}]}\left(\frac{\lambda_L}{1[\mu\mathrm{m}]}\right)^2, \end{aligned} \quad (17)$$

where $\gamma_f = E_b/m\,c^2$ is the Lorentz factor at the final beam energy. The overall length of a linac consisting of periodic structures of an accelerator stage and a coupling section

https://doi.org/10.1017/S0263034612000079 Published online by Cambridge University Press

that installs both beam and laser focusing systems leads to be

$$L_{\text{total}} \simeq \left(L_{\text{stage}} + L_{\text{coupl}}\right)N_{\text{stage}} \approx 589[\text{m}]\frac{E_b}{1[\text{TeV}]}\left(\frac{10^{15}[\text{cm}^{-3}]}{n_p}\right)^{1/2}\left(1+\frac{L_{\text{coupl}}}{L_{\text{stage}}}\right). \quad (18)$$

The laser spot size is bounded by conditions for avoiding bubble formation, $k_p^2 r_L^2/4 > a_L^2/\sqrt{1+a_L^2/2}$ and strong self-focusing, $P_L/P_c = k_p^2 r_L^2\ a_L^2/32 \le 1$, where $P_c = 2(m^2 c^5/e^2)\omega_L^2/\omega_p^2 \simeq 17(n_c/n_p)[\text{GW}]$. These conditions put bounds to the spot size $2.5 \le k_p\ r_L \le 3.8$ for $a_L = 1.5$. Accordingly we choose $k_p r_L = 3$. For a given spot radius,

$$r_L = \frac{\lambda_L}{2\pi}k_p r_L\left(\frac{n_c}{n_p}\right)^{1/2} \approx 510[\mu\text{m}]\left(\frac{10^{15}[\text{cm}^{-3}]}{n_p}\right)^{1/2}, \quad (19)$$

the peak laser power becomes

$$P_L = \frac{k_p^2 r_L^2}{32}a_L^2 P_c \approx 12[\text{PW}]\left(\frac{1[\mu\text{m}]}{\lambda_L}\right)^2\frac{10^{15}[\text{cm}^{-3}]}{n_p}. \quad (20)$$

With the FWHM pulse duration given by

$$\tau_L = \frac{\sqrt{\ln 2}}{\pi}\frac{\lambda_L}{c}k_p\sigma_L\left(\frac{n_c}{n_p}\right)^{1/2} \simeq 930[\text{fs}]\left(\frac{10^{15}[\text{cm}^{-3}]}{n_p}\right)^{1/2}, \quad (21)$$

the required laser pulse energy is obtained as

$$U_L = P\tau_L \approx 11[\text{kJ}]\left(\frac{1[\mu\text{m}]}{\lambda_L}\right)^2\left(\frac{10^{15}[\text{cm}^{-3}]}{n_p}\right)^{3/2}. \quad (22)$$

3. BETATRON OSCILLATION

Beams that undergo strong transverse focusing forces $F_\perp = -\,mc^2 K^2 x_\beta$, in plasma waves exhibit the betatron oscillation, where x_β is the transverse amplitude of the betatron oscillation. From the axial and radial fields, Eqs. (7) and (8), the focusing constant K is given by

$$K^2 \simeq \frac{4k_p^2}{\left(k_p r_L\right)^2}\frac{E_z}{E_0}\sin\Psi, \quad (23)$$

where $\Psi = k_p\ (z - v_p t) + \Psi_0$ is the dephasing phase of the wakefield and Ψ_0 is the injection phase. The envelope equation of the rms beam radius σ_r is given by

$$\frac{d^2\sigma_r}{dz^2} + \frac{K^2}{\gamma}\sigma_r - \frac{\varepsilon_{n0}^2}{\gamma^2\sigma_r^3} = 0, \quad (24)$$

where ε_{n0} is the initial normalized emittance. Assuming the beam energy γ is constant, this equation is solved with the initial conditions $\sigma'_{r0} = (d\sigma_r/dz)_{z=0}$ and $\sigma_{r0} = \sigma_r(0)$ as

$$\sigma_r^2(z) = \frac{C}{\kappa^2} + \frac{1}{\kappa}\sqrt{\frac{C^2}{\kappa^2} - \frac{4\varepsilon_{n0}^2}{\gamma^2}}\sin\left(\kappa z + \phi_0\right), \quad (25)$$

where $\kappa = 2K/\sqrt{\gamma}$ is the focusing strength, $C = 2\sigma'_{r0} + \kappa^2\ \sigma_{r0}^2/2 + 2\varepsilon_{n0}^2/\gamma^2\ \sigma_{r0}^2$ is the constant

$$\tan\phi_0 = \frac{\sigma_{r0}^2 - C/\kappa^2}{2\sigma_{r0}\sigma'_{r0}/\kappa}. \quad (26)$$

The beam envelope oscillates around the equilibrium radius $\bar{\sigma}_r = \sqrt{C}/\kappa$ with the wavelength $2\pi/\kappa = \pi/k_\beta$, where $2\pi/\kappa = \pi/k_\beta$ the betatron wavelength. For the condition $C/\kappa = 2\varepsilon_{n0}/\gamma$ that leads to $\sigma_{r0}^2 = 2\varepsilon_{n0}/\kappa\gamma$ with $\sigma'_{r0} = 0$, the beam propagates at the matched beam radius

$$\sigma_{rM}^2 = \frac{2\varepsilon_{n0}}{\kappa\gamma} = \frac{\varepsilon_{n0}}{k_\beta\gamma} = \frac{\varepsilon_{n0}}{K\sqrt{\gamma}} \approx \frac{r_L\varepsilon_{n0}}{2\sqrt{\gamma}}\left(\frac{E_z}{E_0}\sin\Psi\right)^{-1/2}. \quad (27)$$

4. BEAM DYNAMICS AND RADIATIVE DAMPING

The synchrotron radiation causes the energy loss of beams and affects the energy spread and transverse emittance via the radiation reaction force. The motion of an electron traveling along z-axis in the accelerating force eE_z and the radial force eE_r from the plasma wave evolves according to

$$\frac{du_x}{cdt} = -K^2 x + \frac{F_x^{\text{RAD}}}{mc^2}, \qquad \frac{du_z}{cdt} = k_p\frac{E_z}{E_0} + \frac{F_z^{\text{RAD}}}{mc^2}, \quad (28)$$

where $\mathbf{F}^{\text{RAD}}$ is the radiation reaction force and $\mathbf{u} = \mathbf{p}/mc$ is the normalized electron momentum. The classical radiation reaction force (Jackson, 1999), is given by

$$\frac{\mathbf{F}^{\text{rad}}}{mc\tau_R} = \frac{d}{dt}\left(\gamma\frac{d\mathbf{u}}{dt}\right) + \gamma\mathbf{u}\left[\left(\frac{d\gamma}{dt}\right)^2 - \left(\frac{d\mathbf{u}}{dt}\right)^2\right], \quad (29)$$

where $\gamma = (1+u^2)^{1/2}$ is the relativistic Lorentz factor of the electron and $\tau_R = 2r_e/3c \simeq 6.26\times10^{-24}$ s. Since the scale length of the radiation reaction is much smaller than that of the betatron motion, assuming that the radiation reaction force is a perturbation and $u_z \gg u_x$, the equations of motion Eqs. (28) approximately turn to the following coupled equations,

$$\frac{d^2x}{dt^2} + \left(\frac{\omega_p}{\gamma}\frac{E_z}{E_0} + \tau_R c^2 K^2\right)\frac{dx}{dt} + \frac{c^2K^2}{\gamma}x = 0, \quad (30)$$

and

$$\frac{d\gamma}{dt} = \omega_p\frac{E_z}{E_0} - \tau_R c^2 K^4\gamma^2 x^2. \quad (31)$$

The radiative damping rate is defined by the ratio of the radiated power, $P_s \simeq (2e^2\gamma^2/3m^2c^3)F_\perp^2$ to the electron energy as $\nu_\gamma = P_s/\gamma m\ c^2 \simeq \tau_R\gamma F_\perp^2/m^2c^2$.

Corresponding to the single particle equations Eqs. (30) and (31) with radiation damping, the envelope equation is

https://doi.org/10.1017/S0263034612000079 Published online by Cambridge University Press

written as

$$\frac{d^2\sigma_r}{dz^2}+\left(\frac{k_p}{\gamma}\frac{E_z}{E_0}+\tau_R c K^2\right)\frac{d\sigma_r}{dz}+\frac{K^2}{\gamma}\sigma_r-\frac{\varepsilon_{n0}^2}{\gamma^2\sigma_r^3}=0, \tag{32}$$

and

$$\frac{d\gamma}{dz}=k_p\frac{E_z}{E_0}-2\tau_R c K^4\gamma^2\sigma_r^2. \tag{33}$$

Here we define the transverse emittance,

$$\varepsilon\equiv\sigma_r\frac{d\sigma_r}{dz}=\frac{1}{2}\frac{d\sigma_r^2}{dz}, \tag{34}$$

and consider the matched beam case, defined by Eq. (27) with the normalized emittance ε_n, i.e., $\sigma_r^2=\varepsilon/k_\beta=\varepsilon_n/K\sqrt{\gamma}$, using the following dimensionless variables and parameters; $\zeta\equiv k_p z$, $\Omega(\zeta)\equiv k_p\varepsilon_n$, $\chi\equiv E_z/E_0$ and $K/k_p=\alpha\chi^{1/2}$. The coupled equations on the normalized emittance is obtained as

$$\frac{d^2\Omega}{d\zeta^2}+E(\gamma)\frac{d\Omega}{d\zeta}+F(\gamma)\Omega=0, \tag{35}$$

$$\frac{d\gamma}{d\zeta}=\chi-2\tau_R\omega_p\alpha^3\chi^{3/2}\gamma^{3/2}\Omega, \tag{36}$$

and

$$\frac{d}{d\zeta}\left(\frac{\delta\gamma}{\gamma}\right)=-\left[\frac{\chi}{\gamma}+\tau_R\omega_p\alpha^3\chi^{3/2}\gamma^{1/2}\Omega+2\tau_R\omega_p\alpha^3\chi^{3/2}\gamma^{3/2}\frac{d\Omega}{d\gamma}\right]\frac{\delta\gamma}{\gamma}, \tag{37}$$

where

$$E(\gamma)=\frac{2\alpha\chi^{1/2}}{\gamma^{1/2}}-\frac{\chi}{\gamma}+\tau_R\omega_p\alpha^2\chi+6\tau_R\omega_p\alpha^3\chi^{3/2}\gamma^{1/2}\Omega, \tag{38}$$

and

$$\begin{aligned}F(\gamma)=&-\alpha\frac{\chi^{3/2}}{\gamma^{3/2}}+\tau_R\omega_p\left(\frac{2\alpha^3\chi^{3/2}}{\gamma^{1/2}}-\frac{\alpha^2\chi^2}{\gamma}\right)\\&+\left(6\tau_R\omega_p\alpha^4\chi^2-\tau_R\omega_p\alpha^3\chi^{5/2}\gamma^{-1/2}+2\tau_R^2\omega_p^2\alpha^5\chi^{5/2}\gamma^{1/2}\right)\Omega\\&+2\tau_R^2\omega_p^2\alpha^6\chi^3\gamma\Omega^2.\end{aligned} \tag{39}$$

For given $\chi=E_z/E_0$ and $\alpha=(K/k_p)\chi^{-1/2}$, the normalized emittance, energy and energy spread are obtained by integrating the coupled equations, Eqs. (35)–(37) as a function of $\zeta=k_p+z$, provided with the initial conditions γ_0, $(\delta\gamma/\gamma)_0$, Ω_0 and $(d\Omega/d\zeta)_0$.

5. LASER-PLASMA ACCELERATION BEYOND 1 TEV

Harnessing the state-of-the-art high-energy lasers on the order of 10 kJ and the ongoing development of ultra-intense lasers with the peak power on the order of 10 PW and the pulse duration on the order of 1 ps, we explore the feasibility of accelerating electron beams up to energies much beyond 1 TeV in a realistic scale on the order of tens of kilometers and evolution of the beam qualities such as emittance and energy spread at the final beam energy, using the equations describing the beam dynamics in Section 4. Relying on the state-of-the-art laser-plasma acceleration technologies and/or the conventional radio frequency (RF) linac technologies, we assume the initial electron beam with energy of 1 GeV, relative energy spread of 1%, and bunch duration of 10 fs, which is externally injected from a high-quality electron beam injector into the laser-plasma accelerator stage. According to the scaling formulas described in Section 2, the stage energy gain $W_{\rm stage}=1$ TeV can be achieved in the stage length $L_{\rm stage}\approx 590$ m, which is operated at the plasma density $n_p=10^{15}$ cm^{-3}. With the coupling length between consecutive stages, $L_{\rm coupl}\approx 10$ m, the total length per stage is 600 m and the total linac length at the final beam energy E_b turns out to be $L_{\rm total}[{\rm km}]\approx 0.6E_b$ [TeV]. Making reference to the currently ongoing large-scale collider projects such as international linear collider (ILC) and compact linear collider (CLIC) based on RF accelerator technologies, which reach 47 km at 1 TeV collider and 42 km at 3 TeV collider, here we present the feasibility study of 10–100 TeV class linear accelerators in the scale of 6–100 km, based on laser-plasma accelerators. Table 1 show the underlying parameters of the laser-plasma accelerator for the stage energy gain 1 TeV, which are used as the basis for the present study.

The coupled equations, Eqs. (35)–(37), can be integrated numerically as a function of $\zeta=k_p z$, using the Runge-Kutta algorithm. The results of energy γ, relative energy spread $\delta\gamma/\gamma$, normalized emittance ε_n, and relative radiation loss

Table 1. *Example parameters of a 1 TeV laser-plasma accelerator stage*

Energy gain per stage $W_{\rm stage}$	1 TeV
Injection beam energy E_i	1 GeV
Plasma density n_p	1×10^{15} cm^{-3}
Plasma wavelength λ_p	1056 μm
Accelerating field E_z ($\chi=E_z/E_0$)	1.7 GV/m (0.56)
Focusing constant K/k_p (α)	0.35 (0.47)
Stage length $L_{\rm stage}$ ($L_{\rm coupl}$)	590 m (10 m)
Charge per bunch Q_b (N_b)	1.3 nC (8×10^9)
Matched beam radius σ_{r0} (ε_{n0})	168 μm (2622 μm rad)
Laser wavelength λ_L	1 μm
Laser intensity I_L (a_L)	3×10^{18} W/cm^2 (1.5)
Laser pulse duration τ_L	930 fs
Laser spot radius r_L	510 μm
Laser peak power P_L	12 PW
Laser energy per stage U_L	11 kJ
Plasma channel depth at r_L $\Delta n_c/n_p$	0.44

https://doi.org/10.1017/S0263034612000079 Published online by Cambridge University Press

rate R at the plasma density $n_p = 10^{15}$ cm^{-3} are shown for various initial normalized emittances ε_{n0} as a function of the acceleration distance z in Figure 1. Here the relative radiation loss rate R is defined as the ratio of the radiation loss rate to the acceleration gradient $\chi = E_z/E_0$, i.e.,

$$R(\zeta) \equiv 2\tau_R \omega_p \alpha^3 \chi^{1/2} \gamma^{3/2} \Omega. \tag{40}$$

Figure 2 shows the evolution of these beam parameters for the plasma densities $n_p = 10^{15}-10^{18}$ cm^{-3} as a function of the dimensionless distance $\zeta = k_p z$. In all figures, as the beam energy increases, keeping the radiation loss rate small, the emittance growth initially occurs, while the relative energy spread reduces. This behavior is attributed to conservation of the total phase space volume as a result of the adiabatic properties of the electron beam. After the emittance growth balances with radiative damping of the betatron motion at its maximum, the normalized emittance turns to damping as the radiation loss rate R increases quickly until reaching a constant rate $R_T = 2\tau_R\, \omega_p\, \alpha^3\, \chi^{1/2} \Omega \gamma_T^{3/2} = 2/3$ at the transition energy γ_T, where the radiation loss rate reaches the maximum rate $R \simeq R_T$. It is noted that the R_T is evaluated without regard to the initial condition ε_{n0} and the plasma density n_p. In the energy region $\gamma \geq \gamma_T$, as the radiation loss rate is $R \simeq R_T = 2/3$, the normalized emittance is approximately evaluated as

$$\begin{aligned} \varepsilon_n &= \frac{1}{8\pi r_e^2 n_p} \gamma^{-3/2} \left(\frac{E_z}{E_0}\right) \left(\frac{K}{k_p}\right)^{-3} \\ &\approx 1.8[\mu\text{m}] \left(\frac{E_z}{E_0}\right) \left(\frac{K}{k_p}\right)^{-3} \left(\frac{n_p}{10^{15}[\text{cm}^{-3}]}\right)^{-1} \left(\frac{E_b}{100[\text{TeV}]}\right)^{-3/2} \end{aligned} \tag{41}$$

where E_b is the electron beam energy, as shown in Figures 1d and 2d.

6. DISCUSSIONS AND CONCLUSIONS

We have carried out the feasibility study on laser-plasma acceleration in the multi-TeV regime, where strong betatron radiations dominate the beam dynamics of electrons that lead to radiative damping of the normalized emittance, and the energy spread as a result of synchrotron radiation due to the focusing force in plasma wakefields. The radiative damping effects due to betatron oscillation are quite different from other radiative damping or cooling mechanisms such as synchrotron radiation damping in an electron or positron storage ring (Chao & Tigner, 1999), and the radiative cooling via laser-electron Compton scattering (Telnov, 1997; Huang & Ruth, 1998; Esarey, 2000; Mao *et al.*, 2010). In the electron storage ring, the damping is caused by emission of synchrotron radiation due to the uniform bending fields and by recovering the energy loss only in the longitudinal direction. However, the radiative energy loss limits the highest beam energy, at which the energy loss surpasses the power of recovering it. In the laser-plasma acceleration, the radiative energy loss is proportional to the emittance and does not surpass the acceleration gradient, indicated in Eq. (36),

$$\frac{d\gamma}{d\zeta} = \chi(1 - R_T) \simeq \frac{1}{3}\left(\frac{E_z}{E_0}\right) > 0, \tag{42}$$

for $\gamma \geq \gamma_T$. This implies that the beam energy can be increased without limit due to the radiative loss and the normalized emittance decreases without saturation. However, the net accelerating gradient reduces to one-third of the initial

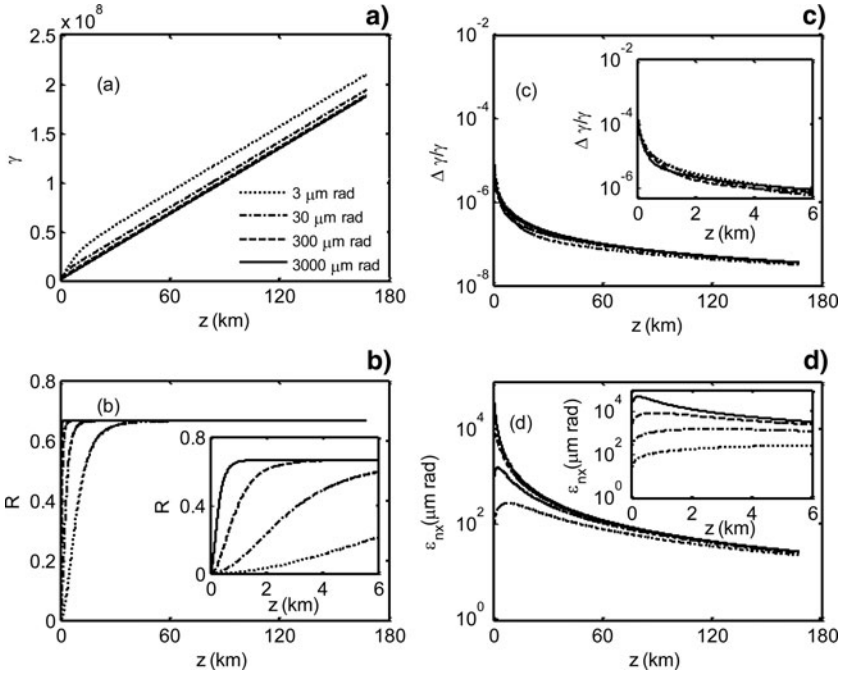

Fig. 1. Evolutions of (**a**) energy γ, (**b**) relative radiation loss rate R, (**c**) relative energy spread $\delta\gamma/\gamma$, and (**d**) normalized emittance ε_n for an electron beam with the initial emittance $\varepsilon_{n0} = 3$, 30, 300, and 3000 μmrad, and the initial energy $E_i = 1$ GeV with initial energy spread $\delta\gamma/\gamma = 0.01$, injected into the plasma channel with density $n_p = 10^{15}$ cm^{-3} as a function of the acceleration distance z. Plotted are numerical integrations of the coupled equations Eqs. (35)–(37) for the accelerating field $E_z = 1.7$ GV/m ($E_z/E_0 = 0.56$), and the focusing constant $K/k_p = 0.35$ ($\alpha = 0.47$).

https://doi.org/10.1017/S0263034612000079 Published online by Cambridge University Press

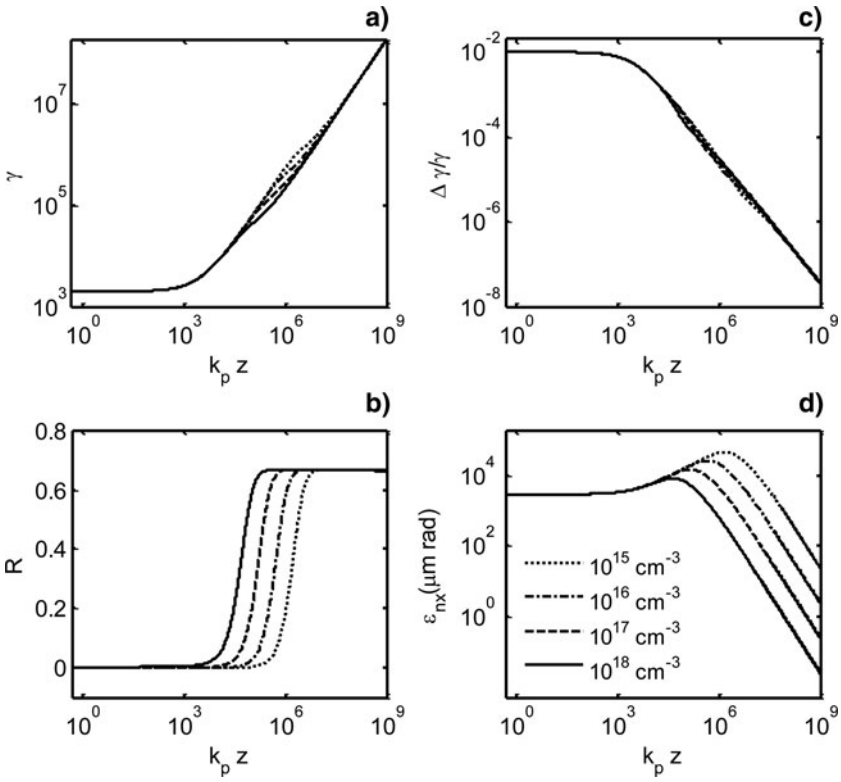

Fig. 2. Evolutions of (**a**) energy γ, (**b**) relative radiation loss rate R, (**c**) relative energy spread $\delta\gamma/\gamma$, and (**d**) normalized emittances ε_n of electron beams with different plasma densities of 10^{15} cm^{-3}, 10^{16} cm^{-3}, 10^{17} cm^{-3}, and 10^{18} cm^{-3}, respectively, as a function of the dimensionless acceleration distance $\zeta = k_p\, z$. The initial conditions of beam energy, normalized transverse emittance and energy spread are $\gamma_0 = 2000$, $\varepsilon_{n0} = 3000$ μm rad and $\delta\gamma/\gamma = 0.01$, respectively.

accelerating gradient due to the betatron radiation loss for $\gamma \geq \gamma_T$ so that three times longer acceleration distance, 180 km, is required to reach the final beam energy 100 TeV.

In a plasma focusing channel, multiple Coulomb scattering between a beam electron and a plasma ion counteracts the radiation damping due to betatron radiation. The damping rate of the normalized emittance is given by

$$\left(\frac{d\varepsilon_n}{dt}\right)_{\rm RAD} \simeq c\frac{d\Omega}{d\gamma}\frac{d\gamma}{d\zeta} = -\frac{c\chi}{6\tau_R\omega_p\alpha^3\chi^{1/2}}\gamma^{-5/2}. \qquad (43)$$

The growth rate for the normalized emittance due to multiple Coulomb scattering (Schroeder *et al.*, 2010) is given by

$$\left(\frac{d\varepsilon_n}{dt}\right)_{\rm SCAT} \simeq \frac{ck_p^2 r_e Z}{K\gamma^{1/2}}\ln\left(\frac{\lambda_D}{R_N}\right), \qquad (44)$$

where Z is the charge state of the ion, $\lambda_D = (T_e/4\pi n_p\, e^2)^{1/2}$ is the Debye length for the plasma temperature T_e eV and R_N is the effective Coulomb radius of the nucleus, which is approximated as $R \approx 1.4A^{1/3}$ fm with the mass number A. The equilibrium emittance is obtained from balancing the radiation damping with the emittance growth due to multiple Coulomb scattering, i.e., $(d\varepsilon_n/dt)_{\rm RAD} + (d\varepsilon_n/dt)_{\rm Scatter} = 0$. Solving this equation with respect to γ gives an estimate of the equilibrium energy $\gamma_{\rm EQ}$ at which the radiative damping reaches the balance with the emittance growth as

$$\gamma_{\rm EQ} = \left(16\pi r_e^3 n_p Z\ln\frac{\lambda_D}{R_N}\right)^{-1/2}\frac{E_z}{E_0}\left(\frac{K}{k_p}\right)^{-1} = \frac{6\times 10^9}{(Z\Lambda)^{1/2}}\frac{E_z}{E_0}\left(\frac{K}{k_p}\right)^{-1}\left(\frac{n_p}{10^{15}[{\rm cm}^{-3}]}\right)^{-1/2}, \qquad (45)$$

where Λ is calculated from

$$\Lambda \approx \frac{1}{24.7}\ln\left(\frac{\lambda_D}{R_N}\right) \approx 1 + 0.047\log\left[\frac{T_e}{10[{\rm eV}]}\left(\frac{n_e A^{2/3}}{10^{15}[{\rm cm}^{-3}]}\right)^{-1}\right].$$

Thus, the equilibrium emittance is estimated as

$$\varepsilon_{n\rm EQ} = 11[{\rm nm}](Z\Lambda)^{3/4}\left(\frac{E_z}{E_0}\right)^{-1/2}\left(\frac{K}{k_p}\right)^{-3/2}\left(\frac{n_p}{10^{15}[{\rm cm}^{-3}]}\right)^{-1}. \qquad (46)$$

For the underlying parameters of the laser-plasma accelerator given by Table 1, the equilibrium emittance becomes $\varepsilon_{n\rm EQ} =$ 71 nm at $\gamma_{\rm EQ} \simeq 9.6\times 10^9$ (4.9 PeV) in a hydrogen plasma with $Z = 1$ and $A = 1$.

The quantum mechanical consideration of radiation damping in the continuous focusing channel results in the minimum normalized emittance (Huang *et al.*, 1995) $\varepsilon_{n\rm min} = \lambda\!\!\!^{-}/2 \simeq 0.2$ pm, where $\lambda\!\!\!^{-} = \hbar/mc$ is the Compton wavelength, which is the fundamental emittance limited by the uncertainty principle, in case no other excitation sources than radiation reaction are present. According to the emittance scaling Eq. (41) in the energy region $\gamma \geq \gamma_T$, this quantum limit may

https://doi.org/10.1017/S0263034612000079 Published online by Cambridge University Press

be achieved at the electron energy $E_b = 2.4 \times 10^{19}$ eV for $n_p = 10^{15}$ cm^{-3}.

ACKNOWLEDGEMENTS

The authors would like to thank T. Tajima for useful discussions. The work has been supported by the National Natural Science Foundation of China (Project Nos. 10834008, 10974214, and 60921004) and the 973 Program (Project Nos. 2011CB808104, 2011CB808100, and 2010CB923203). K. Nakajima is supported by Chinese Academy of Sciences Visiting Professorship for Senior International Scientists (Grant No. 2010T2G02).

REFERENCES

Chao, A.W. & Tigner, M. (1999). *Handbook of Accelerator Physics and Engineering* (Chao, A.W. & Tigner, M., eds.). Singapore: World Scientific.

Clayton, C.E., Ralph, J.E., Albert, F., Fonseca, R.A., Glenzer, S.H., Joshi, C., Lu, W., Marsh, K.A., Martins, S.F., Mori, W.B., Pak, A., Tsung, F.S., Pollock, B.B., Ross, J.S., Silva, L.O. & Froula, D.H. (2010). Self-guided laser wakefield acceleration beyond 1 GeV using ionization-induced injection. *Phys. Rev. Lett.* **105**, 105003/1–4.

Esarey, E. (2000). Laser cooling of electron beams via Thomson scattering. *Nucl. Instr. Meth. Phys. Res.* A **455**, 7–14.

Faure, J., Glinec, Y., Pukhov, A., Kiselev, S., Gordienko, S., Lefebvre, E., Rousseau, J-P., Burgy, F. & Malka, V. (2004). A laser–plasma accelerator producing monoenergetic electron beams. *Nat.* **431**, 541–544.

Faure, J., Rechatin, C., Norlin, A., Lifschitz, A., Glinec, Y. & Malka, V. (2006). Controlled injection and acceleration of electrons in plasma wakefields by colliding laser pulses. *Nat.* **444**, 737–739.

Geddes, C.G.R., Toth, CS., Tilborg, J. van, Esarey, E., Schroeder, C.B., Bruhwiler, D., Nieter, C.J., Cary, J. & Leemans, W.P. (2004). High-quality electron beams from a laser wakefield accelerator using plasma-channel guiding. *Nat.* **431**, 538–541.

Glinec, Y., Faure, J., Pukhov, A., Kiselev, S., Gordienko, S., Mercier, B. & Malka, V. (2005). Generation of quasi-monoenergetic electron beams using ultrashort and ultraintense laser pulses. *Laser Part. Beams* **23**, 161–166.

Hafz, N.A.M., Jeong, T.M., Choi, I.W., Lee, S.K., Pae, K.H., Kulagin, V.K., Sung, J.H., Yu, T.J., Hong, K.H., Hosokai, T.R. Cary, J.R., Ko, D.K. & Lee, J.M. (2008). Stable generation of GeV-class electron beams from self-guided laser–plasma channels. *Nat. Photo.* **2**, 571–577.

Huang, Z.R. & Ruth, R.D. (1998). Laser-electron storage ring. *Phys. Rev. Lett.* **80**, 976–979.

Huang, Z.R., Chen, P. & Ruth, R.D. (1995). Radiation reaction in a continuous focusing channel. *Phys. Rev. Lett.* **74**, 1759–1762.

Jackson, J.D. (1999). *Classical Electrodynamics*. New York: John Wiley & Sons.

Kameshima, T., Hong, W., Sugiyama, K., Wen, X.L., Wu, Y.C., Tang, C.M., Qihua Zhu, Q.H., Gu, Y.Q., Zhang, B.H., Peng, H.S., Kurokawa, S., Chen, Tajima, T., Kumita, T. & Nakajima, K. (2008). 0.56 GeV laser electron acceleration in ablative-capillary- discharge plasma channel. *Appl. Phys. Expr.* **1**, 066001/1–3.

Karsch, S., Osterhoff, J., Popp, A., Rowlands-Rees, T.P., Major, ZS., Fuchs, Z.M., Marx, B., Hörlein, R., Schmid, K., Veisz, L., Becker, S., Schramm, U., Hidding, B., Pretzler, G., Habs, D., Grüner, F., Kraus, F. & Hooker, S.M. (2007). GeV-scale electron acceleration in a gas-filled capillary discharge waveguide. *New J. Phys.* **9**, 415–425.

Kostyukov, I., Pukhov, A. & Kiselev, S. (2004). Phenomenological theory of laser-plasma interaction in "bubble" regime. *Phys. Plasmas* **11**, 5256–5264.

Kotaki, H., Daito, I., Kando, M., Hayashi, Y., Kawase, K., Kameshima, T., Fukuda, Y., Homma, T., Ma, J., Chen, L.M., Esirkepov, T. Zh., Pirozhkov, A.S., Koga, J.K., Faenov, A., Pikuz, T., Kiriyama, H., Okada, H., Shimomura, T., Nakai, Y., Tanoue, M., Sasao, H., Wakai, D., Matsuura, H., Kondo, S., Kanazawa, S., Sugiyama, A., Daido, H. & Bulanov, S.V. (2009). Electron optical injection with head-on and counter-crossing colliding laser pulses. *Phys. Rev. Lett.* **103**, 194803/1–4.

Leemans, W.P., Nagler, B., Gonsalves, A.J., Toth, CS., Nakamura, K., Geddes, C.G.R., Esarey, E., Schroeder, C.B. & Hooker, S.M. (2006). GeV electron beams from a centimetre-scale accelerator. *Nat. Physics* **2**, 696–699.

Liu, J.S., Xia, C.Q., Wang, W.T., Lu, H.Y., Wang, CH., Deng, A.H., Li, W.T., Zhang, H., Liang, X.Y., Leng, Y.X., Lu, X.M., Wang, C., Wang, J.Z., Nakajima, K., Li, R.X. & Xu, Z.Z. (2011). All-optical cascaded laser Wakefield accelerator using ionization-induced injection. *Phys. Rev. Lett.* **107**, 035001/1–4.

Lu, H.Y., Liu, M.W., Wang, W.T., Wang, C., Liu, J.S., Deng, A.H., Xu, J.C., Xia, C.Q., Li, W.T., Zhang, H., Lu, X.M., Wang, C., Wang, J.Z., Liang, X.Y., Leng, Y.X., Shen, B.F., Nakajima, K., Li, R.X. & Xu, Z.Z. (2011). Laser Wakefield acceleration of electron beams beyond 1 GeV from an ablative capillary discharge waveguide. *Appl. Phys. Lett.* **99**, 091502/1–3.

Lu, W., Huang, C., Zhou, M., Mori, W.B. & Katsouleas, T. (2006). Nonlinear theory for relativistic plasmawakefields in the blowout regime. *Phys. Rev. Lett.* **96**, 165002/1–4.

Lundh, O., Lim, J., Rechatin, C., Ammoura, L., Ben-Ismaïl, A., Davoine, X., Gallot, G., Goddet, J-P., Lefebvre, E., Malka, V. & Faure, J. (2011). Few femtosecond, few kiloampere electron bunch produced by a laser–plasma accelerator. *Nat. Phys.* **7**, 219–222.

Malka, V. (2002). Charged particle source produced by laser–plasma interaction in the relativistic regime. *Laser Part. Beams* **20**, 217–221.

Mangles, S.P.D., Murphy, C.D., Najmudin, Z., Thomas, A.G.R., Collier, J.L., Dangor, A.E., Divall, E.J., Foster, P.S., Gallacher, J.G., Hooker, C.J., Jaroszynski, D.A., Langley, A.J., Mori, W.B., Norreys, P.A., Tsung, F.S., Viskup, R., Walton, B.R. & Krushelnick, K. (2004). Monoenergetic beams of relativistic electrons from intense laser–plasma interactions. *Nat.* **431**, 535–538.

Mao, Q.Q., Kong, Q., Ho, Y.K., Che, H.O., Ban, H.Y., Gu, Y.J. & Kawata, S. (2010). Radiative reaction effect on electron dynamics in an ultra intense laser field. *Laser Part. Beams* **28**, 83–90.

Martins, S.F., Fonseca, R.A., Lu, W., Mori, W.B. & Silva, L.O. (2010). Exploring laser-wakefield-accelerator regimes for near-term lasers using particle-in-cell simulation in Lorentz-boosted frames. *Nat. Phys.***6**, 311–316.

McGuffey, C., Thomas, A.G.R., Schumaker, W., Matsuoka, T., Chvykov, V., Dollar, F.J., Kalintchenko, G., Yanovsky, V., Maksimchuk, A. & Krushelnick, K. (2010). Ionization induced trapping in a laser Wakefield accelerator. *Phys. Rev. Lett.* **104**, 025004/1–4.

Michel, P., Schroeder, C.B., Shadwick, B.A., Esarey, E. & Leemans, W.P. (2006). Radiative damping and electron beam dynamics in plasma-based accelerators. *Phys. Rev. E* **74**, 026501/1–14.

Nakajima, K. (2000). Particle acceleration by ultraintense laser interactions with beams and plasmas. *Laser Part. Beams* **18**, 519–528.

Nakajima, K., Deng, A.H., Zhang, X.M., Shen, B.F., Liu, J.S., Li, R.X., Xu, Z.Z., Ostermayr, T., Petrovics, S. Klier, C., Iqbal, K., Ruhl, H. & Tajima, T. (2011). Operating plasma density issues on large-scale laser-plasma accelerators toward high-energy frontier. *Phys. Rev.* **14**, 091301/1–12.

Osterhoff, J., Popp, A., Major, ZS., Marx, B., Rowlands-Rees, T.P., Fuchs, M., Geissler, M., Hörlein, R., Hidding, B., Becker, S., Peralta, E.A., Schramm, U., Grüner, F., Habs, D., Krausz, F., Hooker, S.M. & Karsch, S. (2008). Generation of stable, low-divergence electron beams by laser-wakefield acceleration in a steady-state-flow gas cell. *Phys. Rev. Lett.* **101**, 085002/1–4.

Pak, A., Marsh, K.A., Martins, S.F., Lu, W., Mori, W.B. & Joshi, C. (2010). Injection and Trapping of Tunnel-Ionized Electrons into Laser-Produced Wakes. *Phys. Rev. Lett.* **104**, 025003/1–4.

Pollock, B.B., Clayton, C.E., Ralph, J.E., Albert, F., Davidson, A., Divol, L., Filip, C., Glenzer, S.H., Herpoldt, K., Lu, W., Marsh, K.A., Meinecke, J., Mori, W.B., Pak, A., Rensink, T.C., Ross, J.S., Shaw, J., Tynan, G.R., Joshi, C. & Froula, D.H. (2011). Demonstration of a narrow energy spread, 0.5 GeV electron beam from a two-stage laser Wakefield accelerator. *Phys. Rev. Lett.* **107**, 045001/1–4.

Schmid, K., Buck, A., Sears, C.M.S., Mikhailova, J.M., Tautz, R., Herrmann, D., Geissler, M., Krausz, F. & Veisz, L. (2010). Density-transition based electron injector for laser driven Wakefield accelerators. *Phys. Rev.* **13**, 091301/1–5.

Schroeder, C.B., Esarey, E., Geddes, C.G.R., Benedetti, C. & Leemans, W.P. (2010). Physics considerations for laser-plasma linear colliders. *Phys. Rev.* **13**, 101301/1–11.

Telnov, V. (1997). Laser cooling of electron beams for linear colliders. *Phy. Rev. Lett.* **78**, 4757–4760.

Wang, W.M., Sheng, Z.M. & Zhang, J. (2009). Electron injection into laser wakefields by colliding circularly-polarized laser pulses. *Laser Part. Beams* **27**, 3–7.

Weber, S., Riazuelo, G., Michel, P., Loubere, R., Walraet, F., Tikhonchuk, V.T., Malka, V., Ovadia, J. & Bonnaud, G. (2004). Modeling of laser-plasma interaction on hydrodynamic scales: Physics development and comparison with experiments. *Laser Part. Beams* **22**, 189–195